

# Influence of diffusion, trapping, and state filling on charge injection and transport in organic insulators

Marlus Koehler\*

*Institute of Quantum Electronics, Swiss Federal Institute of Technology, ETH Hönggerberg, CH-8093 Zürich, Switzerland*

Ivan Biaggio

*Department of Physics, Lehigh University, Bethlehem, Pennsylvania 18015, USA*

(Received 23 January 2003; published 21 August 2003)

We examine unipolar charge carrier injection in organic insulators containing traps and sandwiched between two equal Ohmic contacts. We show that diffusion of charge carriers from the contacts plays a key role in the electrical transport of thin organic films with a low concentration of traps. In these systems a significant fraction of trapping states can be filled by diffusion even at zero applied bias. The diffusion-induced filling of traps decreases with increasing thickness of the insulator, which produces a “detrapping transition” in the voltage-thickness curve at constant current. The observation of this transition can be useful to determine the trap density. We demonstrate that the density of free charge carriers at the contacts, compared to the density of trapping states in the solid, determines different regimes of diffusion injection. Finally, we discuss how the density of available conducting states in the organic insulator can constrain the charge carrier injection and review the consequences of this effect on the electrical properties of a device.

DOI: 10.1103/PhysRevB.68.075205

PACS number(s): 72.10.Bg, 72.20.Fr, 73.40.Ns, 85.60.-q

## I. INTRODUCTION

The use of organic materials for electronics applications such as organic light emitting diodes and organic field effect transistors critically depends on charge injection from a metallic contact. Despite the fact that these systems have attracted much attention in recent years, the physical processes underlying the injection and transport of charge carriers in organic solids and their influence on the electrical properties of devices are still not well understood. A better understanding of the basic principles involved in device operation is necessary to improve efficiency, stability, and lifetime, and to develop predictive guidelines that can be used to project what modifications are necessary to optimize a device for a specific application. Moreover, predicting the electrical properties of devices based on organic insulators under different conditions can give valuable informations about the use of those devices as a tool to investigate different regimes of electrical conduction in organic materials.

In recent current-voltage measurements on tris (8-hydroxyquinoline) ( $\text{Alq}_3$ ) with Mg contacts, which were performed in ultrahigh vacuum (UHV),<sup>1,2</sup> a trap-filling transition and a space-charge limited current following the Mott-Gurney law<sup>3,5</sup> were observed, implying a very low injection barrier at the Mg/ $\text{Alq}_3$  interface.<sup>1,2</sup> It is then a small conceptual step to go from a low injection barrier to no barriers. How will Ohmic contacts influence the electrical properties of devices based on injection in insulators? This question is also interesting in general because a better injection of charge carriers from the contacts is needed in order to obtain larger current densities at low applied voltages, with the ultimate injection efficiency expected for an Ohmic contact between organic insulator and metal contact. High injected charge carrier densities will be one of the requirements of any future electrically pumped organic laser, which is another motivation to study the electrical properties of an insu-

lator sandwiched between Ohmic contacts.

A first simple effect of Ohmic contacts has maybe already been observed in Refs. 1 and 2. There, a sizeable current was detected even at very low applied fields, despite the exceptional purity of the system studied. This current could be due to charge carriers that enter the organic insulator through diffusion from the Ohmic contacts. In this work we explore this and other more complex effects caused by the diffusion of carriers from Ohmic contacts. Examples of effects that are more difficult to predict, and that we will discuss in this work, are the occurrence of trap filling and the dependence of the electrical characteristics from the thickness of the organic insulator.

We first review the existing theories on charge injection and transport in insulators. When charge carriers are injected into an insulator by an applied electric field, the injected space-charge decreases the electric field at the injecting surface and can give rise to a space-charge-limited current (SCLC). An approximate theory of SCLC in a trap-free insulator was proposed by Mott and Gurney<sup>3,4</sup> and later extended by Rose,<sup>4</sup> Lampert and Mark,<sup>5</sup> and others<sup>5,6</sup> to describe currents limited by the space-charge confined in a single discrete energy level and in localized states with a distribution in energy. The simplified SCLC theory, which is usually applied to model the current-voltage ( $I$ - $V$ ) characteristics of organic devices,<sup>7-11</sup> neglects the role of the diffusion currents and the possible constraints introduced by the available density of free carriers at the contacts. These simplifications, associated to the commonly used boundary condition that the electric field vanishes at the cathode interface, leads to an incorrect description of the space-charge profile near the electrodes. Moreover, the charge injected by diffusion from the contacts can induce a high concentration of free carriers in the whole bulk of the insulating material even without any applied voltage. This effect can be significant in organic thin film devices where the active layer has thick-

nesses of the order of 100 nm or less.<sup>12</sup> In these systems the simplified theory cannot be valid, specially at low applied voltages. Here we show that the simple theory neglecting diffusion is not a good approximation to treat the one-carrier injection problem in thin insulators with a low concentration of traps. Because of the diffusion-induced filling of the trap states, the use of the simple theory to interpret experimental data can severely underestimate important parameters of the organic solid, such as the density of traps or the energetic depth of the trap distribution.

The exact theory for the one-carrier SCLC including diffusion, even in the case of a trap free insulator, is extremely complex because it involves the solution of nonlinear differential equations. Approximate analytical solutions<sup>13,14</sup> and numerical treatments<sup>15-18</sup> of the exact theory have been reported in the literature, but most of them have been proposed to describe the charge carrier transport in inorganic crystals<sup>15-17</sup> (for a review on numerical models of electrical transport in organic insulators see Ref. 19 and the references cited therein). Moreover, the works reported up to now in the literature did not study in detail an important phenomenon that is present in a system formed by an insulator containing traps and sandwiched between two Ohmic contacts: the filling of the trapping states by diffusion of carriers from the contacts and its consequences on the electrical properties of the device. Here we demonstrate that this process cannot be ignored because it determines different regimes of charge carrier conduction.

In the following we analyze the current induced by injection of one type of charge carrier while including diffusion and a possible limited density of states at the injection interface. We present the mathematical formalism, as well as the assumptions we used to simplify the numerical calculations. We then apply this formalism to the simple case of one discrete trap level in the insulator, from which the most important features of the system and a description of the influence of diffusion and state filling is derived. Finally, we extend the numerical calculations to the situation in which there is an exponential trap distribution in the organic insulator. This is a better description, compared to the single trap case, to study the electrical properties of solids with a large degree of structural disorder. When presenting numerical results, we will use a set of parameters typical of organic devices such as those using magnesium as metallic contacts and tris (8-hydroxyquinoline) ( $\text{Alq}_3$ ) as active layer. We will show that the decreased influence of diffusion with increasing insulator thickness produces a “detrapping transition” in the voltage-thickness curve at constant current. In the detrapping region the voltage depends strongly on the thickness due to the rapidly varying concentration of empty trap states that limit the charge mobility.

## II. THEORY

We consider the one-dimensional problem of an insulator sandwiched between two Ohmic metal contacts at  $x=0$  and  $x=L$ . The one-carrier space-charge-limited current in steady-state is defined by the current flow equation, the Gauss equation, and the equation that relates the density of

trapped carrier to the density of free-carrier. Without loss of generality we assume that the injected charge carriers are electrons and that the insulator is free of carriers generated by doping, although we do allow for the presence of energy levels in its band gap that can act as trap centers. The current-flow equation is

$$j = qn(x)\mu E - qD(dn/dx) = \text{const}, \quad (1)$$

where  $q$  is the unit charge,  $n$  is the density of free charge carriers,  $\mu$  is the electron mobility, and  $E$  is the electric field. In this work we assume that  $\mu$  does not depend on  $E$  in order to focus on the effects of diffusion and trapping that we want to study.  $D$  is the electron diffusion constant which is related to the carrier mobility by  $D = (kT/q)\mu$ .

The Gauss equation is

$$\frac{\epsilon\epsilon_0}{q} \frac{dE}{dx} = n(x) + \sum_i n_{t,i}(x), \quad (2)$$

where  $\epsilon$  is the dielectric constant of the insulator and  $n_{t,i}$  is the density of carriers trapped into the  $i$ th trap level. The summation over  $i$  accounts for the presence in the organic material of traps with different trapping properties. For each trap type  $i$ , the total available trap density  $N_{t,i}$ , the density of occupied traps  $n_{t,i}$ , and the free carrier density  $n$  are related by the detailed balance principle  $\partial n_{t,i}/\partial t = \gamma_i n(N_{t,i} - n_{t,i}) - \beta_i n_{t,i}$ , where  $\gamma_i$  and  $\beta_i$  are parameters related to the capture and emission rate of the  $i$ th set of traps, respectively. Assuming steady state between emission and capture at every coordinate  $x$  one finds

$$n_{t,i}(x) = \frac{N_{t,i}}{1 + [N_{e,i}/n(x)]}, \quad (3)$$

where  $N_{e,i} = \beta_i/\gamma_i$  has the units of a density and is characteristic of a particular trap type. It decreases with the thermal activation energy of the trap (i.e., its energetic “depth” in the band gap).

To approximate the different kinds of trap levels that are found in amorphous systems it is possible to consider a distribution of traps with different thermal excitation energies. In this case the quantities in Eq. (3) must be replaced with the corresponding quantities belonging to a continuous variation of thermal excitation energy. Specifically,  $N_{t,i}$  is replaced by  $g(\mathcal{E})$ , the density of localized states per unit of energy ( $\mathcal{E}=0$  corresponds to the energy of the lowest unoccupied conducting state<sup>10</sup>), and  $N_{e,i}$  is replaced by  $N_e(\mathcal{E}) = \mathcal{N}\exp(-\mathcal{E}/kT)$ <sup>5</sup>. The total density of trapped electrons  $n_t(x) = \sum_i n_{t,i}(x)$  in Eq. (2) is then calculated by replacing the summation over  $i$  with an integration

$$\begin{aligned} n_t(x) &= n(x) \int_0^{\mathcal{E}_F} \frac{d\mathcal{E} g(\mathcal{E})}{n(x) + \mathcal{N}\exp(-\mathcal{E}/kT)} \\ &= \int_0^{\mathcal{E}_F} \frac{d\mathcal{E} g(\mathcal{E})}{1 + \exp[-(\mathcal{E} - \mathcal{E}_F)/kT]}, \end{aligned} \quad (4)$$

where  $\mathcal{E}_F$  is determined by the density of free electrons or  $\mathcal{E}_F(x) = kT \ln[\mathcal{N}/n(x)]$ .

Below we will describe both a single trap level described by Eq. (3) and a distribution of traps described by Eq. (4) for the case when the trap density  $g(\mathcal{E})$  is an exponential function of the excitation energy  $\mathcal{E}$ .

We assume that the interfaces between the contacts and the organic material are symmetric so that the density of free electrons at the two device boundaries are equal. Equations (1), (2), and (3) [or (4), in case of a distribution of traps] are then solved numerically for a given value of  $j$ , using the boundary conditions  $n(0)=n(L)=n_0$ , where  $n(0)$  is the density of free electrons at the cathode interface ( $x=0$ ), and  $n(L)$  the density of free electrons at the anode interface ( $x=L$ ).  $n_0$ ,  $N_{e,i}$ , and  $\mathcal{N}$  are assumed to be constants independent from the applied field or the current density.

It is useful to discuss the meaning of the boundary condition  $n(0)=n(L)=n_0$ . If the density of states available for conduction in the insulator was much larger than the density of states in the metal, then  $n_0$  would necessarily correspond to the free-electron density in the metal. But in general, and especially for organic insulators, one can expect that the density of conduction states in the insulator is much smaller than the electron density in the metallic contact. In the absence of any energy barrier at the metal insulator interface we can assume that all conduction states that are energetically accessible to the metal electrons will be filled in contact with the metal. In this case  $n_0$  corresponds to the density of energetically available conduction states in the insulator, and it is a property of the insulator itself, of its energy structure, and of its alignment with the Fermi energy in the metal. As will be shown below, the density of available conducting states can be probed by determining  $n_0$  from the current-voltage characteristics at high applied voltages. Further, in Sec. III(b) we demonstrate that states exponentially distributed in energy in the gap of the insulator (introduced, e.g., by structural disorder) can be filled by diffusion of carriers from the contacts. If  $\mathcal{N}=n_0$ , all the states near the contacts are occupied, resulting in the accumulation of a reservoir of injected carriers in the vicinities of the solid's interfaces. We will show that this reservoir can be naturally formed even without the presence of a dipole layer between the metal and the organic solid to lower the energies of the molecules near the interfaces.<sup>20</sup>

### III. RESULTS AND DISCUSSION

#### A. Single trap level

In this section we analyze the effect of electron diffusion from the contacts in the presence of one trap level in the insulator [ $i=1$  in Eq. (2)] with the same concentration  $N_t = 2 \times 10^{22} \text{ m}^{-3}$  but with different emission properties described by  $N_e$ .

Figure 1 shows the spatial profiles of the free-charge carrier density and the fraction of filled traps along an insulator at a constant current ( $j = 10^{-3} \text{ A/m}^2$ ). The curves are plotted for three insulator thicknesses, and they are calculated for two values of the boundary conditions  $n(0)=n(L)=n_0$  at the interfaces:  $n_0 = 10^{22} \text{ m}^{-3}$  in Fig. 1(a) and  $n_0 = 10^{26} \text{ m}^{-3}$  in Fig. 1(b). In both cases  $N_e = 10^{18} \text{ m}^{-3}$ .

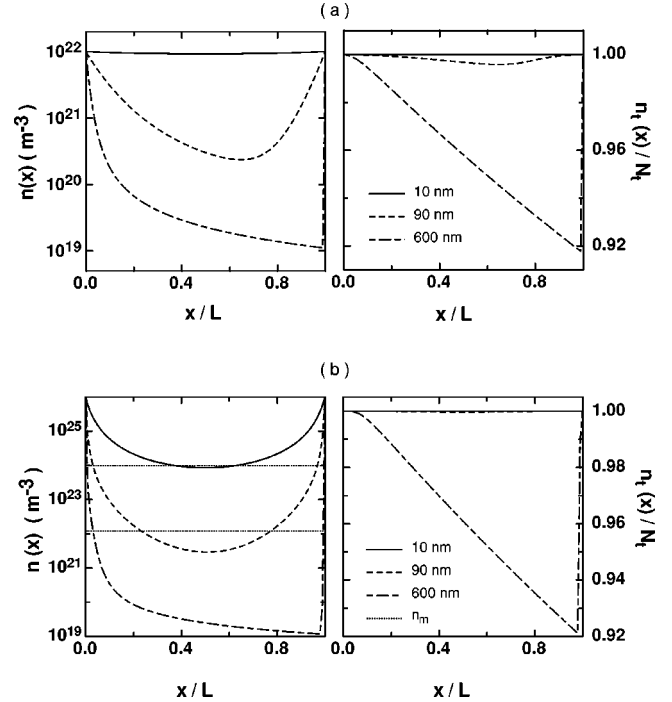


FIG. 1. Free-electron density  $n(x)$  and the corresponding fraction of filled traps  $n_i(x)/N_t$  at a constant current density  $j = 10^{-3} \text{ A m}^{-2}$  for different insulator thicknesses  $L$ . In (a)  $n_0 = 10^{22} \text{ m}^{-3}$  (low injection regime), while in (b)  $n_0 = 10^{26} \text{ m}^{-3}$  (high injection regime). The dotted lines in (b) are given by  $n_m = 2\pi^2 \epsilon \epsilon_0 kT / q^2 L^2$ . The other parameters used to plot this figure are  $N_t = 2 \times 10^{22} \text{ m}^{-3}$ ,  $\mu = 10^{-11} \text{ m}^2 \text{ V}^{-1} \text{ s}^{-1}$ ,  $\epsilon = 3.5$ ,  $N_e = 10^{18} \text{ m}^{-3}$ , and  $j = 10^{-3} \text{ A m}^{-2}$ .

With the help of Fig. 1 it is possible to define two regimes of diffusion injection; the low injection regime, when  $n_0 \leq N_t$  [Fig. 1(a)], and the high injection regime, when  $n_0 > N_t$  [Fig. 1(b)].

In the low injection regime, the density profile of free electrons becomes spatially homogenous (assuming a value  $n_0$ ) when the thickness of the insulator becomes smaller than a characteristic length  $x_0 = [2\epsilon \epsilon_0 kT / (q^2 n_0)]^{1/2}$  [Ref. 14] (taking  $n_0 = 10^{22} \text{ m}^{-3}$ ,  $x_0 \approx 30 \text{ nm}$ ). For thicker devices the free electron density is larger near the contacts and it becomes asymmetric with increasing thickness. For thick insulators the applied field is stronger near the exit contact and diffusion is less important there. Note that near  $x=L$  the electron density has a very sharp increase to reach  $n_0$  at the contact, but that the width of this transition can become very small. A sharp gradient of density in the vicinities of the anode and, consequently, a high diffusion current, is necessary to counterweight the high drift current in this region so that, from Eq. (1),  $j$  remains small. The characteristic length  $x_0$  identifies the thickness at which the transition from a homogenous, diffusion-dominated electron density to a nonhomogenous electron density occurs in the low-injection regime.  $x_0$  is associated to the distance that the carriers can penetrate within the insulator at zero bias until the dipole electric field near the interfaces, created by the charges' displacement, is strong enough to stop the diffusion process. It has the same mathematical definition as the classic Shottky

barrier width in a metal/semiconductor contact at zero current, with  $n_0$  replacing the semiconductor's doping density,<sup>21</sup> and it also has a form similar to the Debye length.

In the high injection regime,  $x_0$  is so small that the condition  $L \ll x_0$  cannot be satisfied even for very thin devices. In this regime, thin insulator thicknesses are characterized by a spatial electron distribution that is practically symmetric with respect to the plane where  $x=L/2$ , but that never becomes spatially homogenous. The density profile of free electrons becomes symmetric when the thickness of the insulator becomes smaller than a characteristic length  $L_{cr} = (2\pi^2 \epsilon \epsilon_0 kT / q^2 N_t)^{1/2}$  (taking  $N_t = 2 \times 10^{22} \text{ m}^{-3}$ ,  $L_{cr} \approx 70 \text{ nm}$ ). When  $L < L_{cr}$ , the minimum electron density reached at  $x=L/2$  can be well approximated by its zero-current value  $n_m = N_t (L_{cr}/L)^2 = 2\pi^2 \epsilon \epsilon_0 kT / q^2 L^2$ .<sup>14</sup> Numerical values of  $n_m$  are identified by dotted horizontal lines in Fig. 1(b). It is important to note that under these circumstances the density of free carriers in the middle of the insulator does not depend on  $n_0$ , but only on the thickness  $L$  and temperature  $T$  of the insulator.<sup>14,22</sup> The free-electron density minimum decreases with the square of the thickness until  $n_m \approx N_t$  and  $L \approx L_{cr}$ . The characteristic length  $L_{cr}$  identifies the thickness at which the transition from a symmetric diffusion dominated electron density to an asymmetric electron density occurs in the high injection regime. Above  $L_{cr}$  diffusion processes are increasingly less important.

From Fig. 1 one can also see that the traps are almost completely filled for very thin devices in both regimes of injection. The solid behaves like a trap-free insulator when  $L < x_0$  or  $L < L_{cr}$ . With increasing thickness, the occupation fraction of the traps decreases and has a minimum in the region near the exit contact. The charge transport becomes then limited by the filling of these empty traps [see Fig. 2(a)]. But it is interesting to note that in the trap-filled region at small thicknesses the resistivity of the device is determined by  $n_0$  in the low-injection regime, and by  $n_m$  in the high-injection regime. As a consequence, the voltage required to drive a given current through the device has a completely different thickness dependence in the two cases.

Figure 2 shows the calculated voltage-thickness ( $V$ - $L$ ) characteristics at constant current and the current-voltage ( $I$ - $V$ ) characteristics for the high- and the low-injection regimes, corresponding to the two different boundary conditions for  $n_0$  used in Fig. 1.

Let us first look at the low-thickness limits in Fig. 2(a). In the low injection regime,  $x_0$  is high and the free charge profile becomes increasingly homogeneous with decreasing  $L$ . For very thin devices ( $x_0 \gg L$ ), the electron density along the solid is almost constant and equal to  $n_0$ , so that the dashed curve in Fig. 2(b) tends to follow the simple linear behavior  $V = (j/q\mu n_0)L$  when  $L \rightarrow 0$  (dotted line in Fig. 2). But for very thin insulators in the high injection regime the thickness dependence of the voltage can be approximated by  $V = (j/q\mu n_m)L = (qj/2\pi^2 \mu \epsilon \epsilon_0 kT)L^3$ , which is plotted as a dotted line in Fig. 2(b). Approximating the nonhomogenous free carrier density by the value at its minimum leads to a slightly too high voltage at the same thickness, but accu-

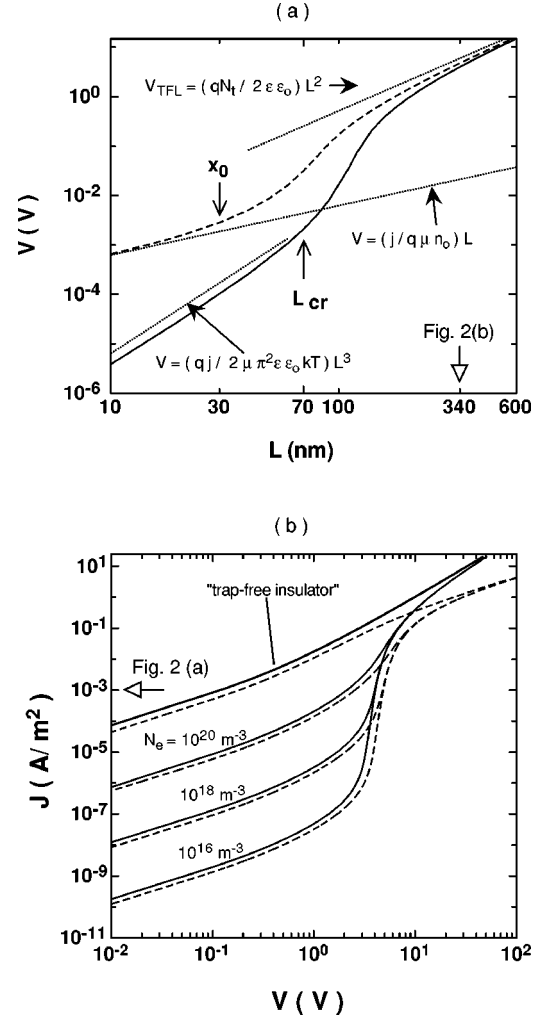


FIG. 2. Electrical properties of an insulator with a single trap level in the low-injection ( $n_0 = 10^{22} \text{ m}^{-3}$ , dashed curves) and the high-injection ( $n_0 = 10^{26} \text{ m}^{-3}$ , solid curves) regimes. (a) Voltage vs thickness for a current density  $j = 10^{-3} \text{ A m}^{-2}$ . The dotted curves correspond to analytical approximations for small and large thicknesses. (b) Current density vs voltage for a thickness  $L = 340 \text{ nm}$ . Apart from the thickness of the insulator, this figure shares the same parameters as Fig. 1.

rately predicts the thickness dependence of the voltage. The voltage varies with the third power of the thickness in the interval  $x_0 < L \leq L_{cr}$ .

These results demonstrate that there is a regime of charge carrier injection in which the bulk density of free electrons varies with the square of the solid's thickness even in the presence of trapping states (and not only in a trap-free solid as it was demonstrated before<sup>14</sup>). It is also very interesting to observe that insulators with the same thicknesses and satisfying the relation  $x_0 < L < L_{cr}$  have almost the same density of free carriers in the bulk, regardless of the values of  $n_0$ ,  $\mu$ , or  $N_t$ .

As the thickness of the insulator increases, the density of filled traps in the bulk of the insulator decreases (see Fig. 1). Hence, for  $L > x_0$  (low injection regime), or  $L > L_{cr}$  (high injection regime), the voltage starts to increase rapidly with thickness due to a "detrapping" transition (in opposition to

the trap-filling process observed in the  $I$ - $V$  curves) induced by the decrease of electrons that have diffused into the bulk of the insulator. This goes on until  $L \gg x_0$  (low injection regime) or  $L \gg L_{cr}$  (high injection regime), when partial trap filling is caused by the trap-density injected by the applied field, as in the conventional SCLC theory with a single trap level.<sup>5,6</sup> Because of the current density that was chosen to plot Fig. 2(a) the density of free carriers near the exit contact never becomes high enough to fill all the traps, and the curves in Fig. 2(a) describe the voltage at which the trap-filling transition occurs in a current-voltage measurement. For large thicknesses, the continuous and the dashed curves of Fig. 2(a) tend then towards the same value and increase with the square of the insulator's thickness. However, this result is only qualitatively in accordance with the simple SCLC theory, which predicts that the trap-filling threshold voltage varies with  $V_{TFL} = (qN_t/2\epsilon\epsilon_0)L^2$ .<sup>6</sup> There is a quantitative discrepancy between the diffusion included and the diffusion neglected  $V_{TFL}$  even for relatively thick devices. For example, taking the parameters of Fig. 2(b) and applying the above relation, the TFL threshold voltage is approximately 6 V, whereas the rise of the current in the curves of Fig. 2(b) occurs at around 3 and 4 V, depending on  $n_0$ .

Figure 2(b) shows the  $I$ - $V$  characteristics predicted for an insulator thickness beyond the detrapping transition of Fig. 2(a), so that the traps are almost empty at low voltages and a trap-filling transition is observed. At low voltages the zero current density profile of the free electrons injected by diffusion is not affected by the applied field and an Ohmic regime ( $j \propto V$ ) is observed<sup>15,16</sup> even in the absence of intrinsic charge carriers in the insulator. This result implies that a relatively small resistivity can be observed even in a highly pure thin insulator once it is sandwiched between two Ohmic contacts.

At higher voltage there is a smooth transition from the Ohms law regime to a steep current increase caused by trap filling. For high values of  $n_0$  (solid curves), the  $I$ - $V$  characteristics at high voltages is controlled by the space-charge in the bulk of the material and is given by the Mott-Gurney law, with the current increasing as the square of the voltage. Because of the boundary conditions which do not allow the charge carrier density to grow past the  $n_0$  maximum set by the boundary conditions this behavior is not expected to go on at even higher voltages. When the injected carrier density in the vicinity of the exit contact starts becoming comparable to  $n_0$ , the carrier density in the insulator saturates at  $n_0$ , and the  $I$ - $V$  characteristics must undergo a transition to a linear regime given by  $j_0 = \mu n_0 q V / L$ . This high-voltage linear regime is seen in Fig. 2(b) for the dashed curves corresponding to a small  $n_0$ . There the linear regime is reached immediately after the trap-filling transition and the Mott-Gurney law never becomes visible. The observation of an Ohmic regime at high voltages can be used to determine  $n_0$  in systems where the charge carrier injection at the metal/solid interface is limited by the poor density of available conducting states in the organic material compared to the density of free electrons in the metal.

The influence of traps with different trapping cross sections and thermal excitation energies can be seen in the

curves plotted in Fig. 2(b) for different values of  $N_e$ . Deeper traps that capture electrons more efficiently and held them trapped for a longer time before thermal excitation are characterized by small values of  $N_e$  and they give rise to much lower currents at low voltages.

### B. Traps distributed exponentially in energy

A practical approximation for the distribution of trap levels that is found in amorphous systems is to use a trap density that increases exponentially for decreasing thermal excitation energies

$$g(\mathcal{E}) = \frac{N_t}{kT_c} \exp(-\mathcal{E}/k_B T_c), \quad (5)$$

where  $k_B$  is Boltzmann's constant and  $T_c$  is a temperature that characterizes the energetic depth of the trap distribution. Such a distribution has been often used in the past to model dispersive charge transport.<sup>23-25</sup> It constitutes a useful representation for many different trap levels all smeared out in energy.<sup>5</sup>

Applying Eq. (5) and assuming a broad distribution so that  $T_c \gg T$ , we can simplify Eq. (4) and write

$$n_t(x) \approx \frac{N_t}{kT_c} \frac{n(x)}{\mathcal{N}} \int_0^{\mathcal{E}_F} d\mathcal{E} \exp\left[-\frac{\mathcal{E}}{k} \left(\frac{T-T_c}{T_c T}\right)\right] + \frac{N_t}{kT_c} \int_{\mathcal{E}_F} d\mathcal{E} \exp\left[-\frac{\mathcal{E}}{kT_c}\right], \quad (6)$$

which can be integrated to give

$$n_t(x) = N_t \left[ \frac{l}{l-1} \left(\frac{n(x)}{\mathcal{N}}\right)^{1/l} - \frac{1}{l-1} \frac{n(x)}{\mathcal{N}} \right], \quad (7)$$

where  $l = T_c/T$ .

Below, we present the numerical solution of Eqs. (1), (2), and (7), and we discuss the corresponding current-voltage characteristics. It will be useful to compare our numerical results to the Mark-Helfrich equation<sup>5</sup>

$$j = \mathcal{N} \mu q^{(1-l)} \left[ \frac{\epsilon \epsilon_0 l}{N_t (l+1)} \right] \left( \frac{2l+1}{l+1} \right)^{(l+1)} \frac{V^{(l+1)}}{L^{(2l+1)}}. \quad (8)$$

This expression can be derived when diffusion effects are neglected and by assuming  $n_t(x) \gg n(x)$  in Eq. (2). That is, it is valid when the majority of injected carriers are trapped. It predicts an  $(l+1)$ -power law variation of the current with the applied voltage and is commonly used to explain the current-voltage characteristics measured in a number of organic and inorganic solids.<sup>6</sup>

The zero-bias Fermi energy profiles along the insulator with an exponential distribution of traps and for  $l=10$  are shown in Fig. 3(a) for two values of the total trap density  $N_t$ . In Fig. 3(b) we also plot the fraction of localized states per unit of energy  $g(\mathcal{E}) \times kT_c / N_t$ . Because of the high concentration of free carriers at the metallic contacts a great fraction of the localized states are filled in the vicinities of the electrodes (in fact, for the high injection regime, all trapping

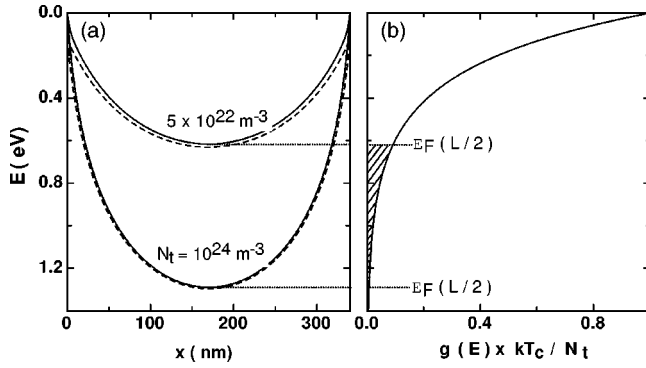


FIG. 3. Distribution of trap filling in an insulator at zero bias in the low injection regime ( $n_0 = 10^{23} \text{ m}^{-3}$ , dashed curves) and in the high-injection regime ( $n_0 = 10^{25} \text{ m}^{-3}$ , solid curves). (a) Energy of the occupied traps with the lowest thermal excitation energy inside a 340 nm thick insulator [same thickness as in Fig. 2(a)] for two values of the total trap density  $N_t = 5 \times 10^{22} \text{ m}^{-3}$  and  $N_t = 10^2 \times 4 \text{ m}^{-3}$ . (b) Plot of the thermal excitation energy vs the corresponding trap density. The filled region and the  $\mathcal{E}$  values marked with  $\mathcal{E}_F$  highlight the fraction of filled states at  $x = L/2$ . Other parameters used to calculate this figure are  $\mathcal{N} = 10^{25} \text{ m}^{-3}$ ,  $\mu = 10^{-11} \text{ m}^2 \text{ V}^{-1} \text{ s}^{-1}$ ,  $l = 10$ , and  $\epsilon = 3.5$ .

states are filled near the interfaces). The fraction of filled states decreases with increasing distance from the contacts, but for the insulator with a low concentration of traps, this fraction remains considerably high even in the bulk [at  $x = L/2$ , the filled fraction of  $g(\mathcal{E}) \times kT_c / N_t$  is around 10%]. With increasing  $N_t$  the variation of the degree of trap filling near the interfaces becomes sharper and the maximum value of the Fermi energy  $\mathcal{E}_F$  higher. In this situation the density of filled states decreases dramatically with increasing distance from the electrodes so that almost all states in the bulk are empty. These states will be filled only when the external electric field is applied.

Figure 4(a) shows the  $I$ - $V$  characteristics of an insulator for different values of the characteristic temperature  $T_c$ . The parameters  $n_0$  and  $L$  are the same as for Fig. 3 and  $N_t = 5 \times 10^{22} \text{ m}^{-3}$ . As in the case of a single trap level, the  $I$ - $V$  curve follows a diffusion induced Ohms law at low voltages up to the rising of the current due to trap filling. But in contrast to the single level case, the rising of the current is less abrupt and can be approximated by a power law in the high voltage range.

It is very important to note that this is only in qualitative accord with the prediction of Eq. (8) because the value of the exponent is significantly lower than the value predicted by Eq. (8). As an example, taking the curve calculated for  $T_c = 1800 \text{ K}$  ( $l = 6$ ) in Fig. 4(a), the slope obtained from a power-law fitting of the trap filling region is 3.93. But Eq. (8) predicts a slope of 7 in this region. This discrepancy is due to the filling of the levels with higher thermal excitation energy (“deep levels”), without any applied bias, with carriers injected by diffusion from the contacts (see Fig. 3). Hence, when the  $I$ - $V$  characteristic is fitted using the conventional SCLC theory (which considers that the trap filling processes starts only when the external electric field is applied) the distribution of discrete states will appear to be more “shal-

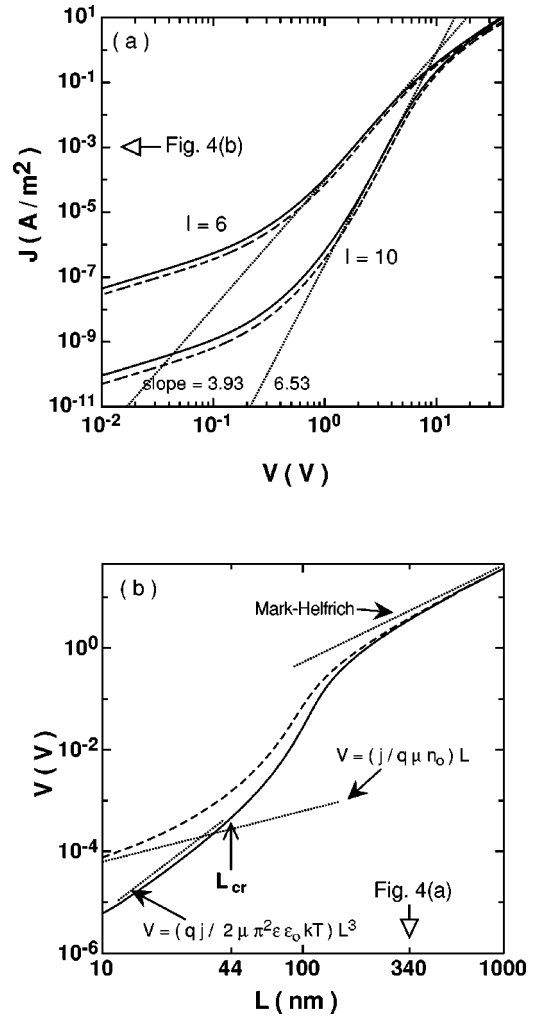


FIG. 4. Electrical properties of a solid with an exponential distribution of traps in the low injection regime ( $n_0 = 10^{23} \text{ m}^{-3}$ , dashed curves) and in the high-injection regime ( $n_0 = 10^{25} \text{ m}^{-3}$ , solid curves) for a low total trap density with  $N_t = 5 \times 10^{22} \text{ m}^{-3}$ . (a) Current-voltage characteristics ( $I$ - $V$ ) of a device with two different trap distributions characterized by  $l = T_c/T = 6$  and  $l = 10$ . (b) Voltage-thickness ( $V$ - $L$ ) characteristics at constant current density ( $j = 10^{-3} \text{ A m}^{-2}$ ) and for  $l = 10$ . All other parameters are the same as for Fig. 3.

low” (lower  $l$ ) than it really is. This effect can lead to significant errors in the determination of  $T_c$  using Eq. (8).

Finally, in the “trap-filled” region at higher voltages the situation is again similar to what is observed for a single trap level. The  $I$ - $V$  characteristics approaches the Mott-Gurney law when  $n_0$  is high, or follows an Ohms law determined by the density of electrons available at the injecting contact  $j_0 = qn_0V/L$  when  $n_0$  is small.

The  $V$ - $L$  characteristics at a constant current for the device in Fig. 4(a) is shown in Fig. 4(b). The parameters are the same as for the curve with  $T_c = 3000 \text{ K}$  ( $l = 10$ ) in Fig. 4(a), with a current density  $j = 10^{-3} \text{ A m}^{-2}$ . The characteristic length for the low-injection regime is  $x_0 \approx 10 \text{ nm}$ . The corresponding length for the high-injection regime is  $L_{cr} \approx 44 \text{ nm}$ . Analytical voltage-thickness approximations are again represented by dotted lines. For small thicknesses, the

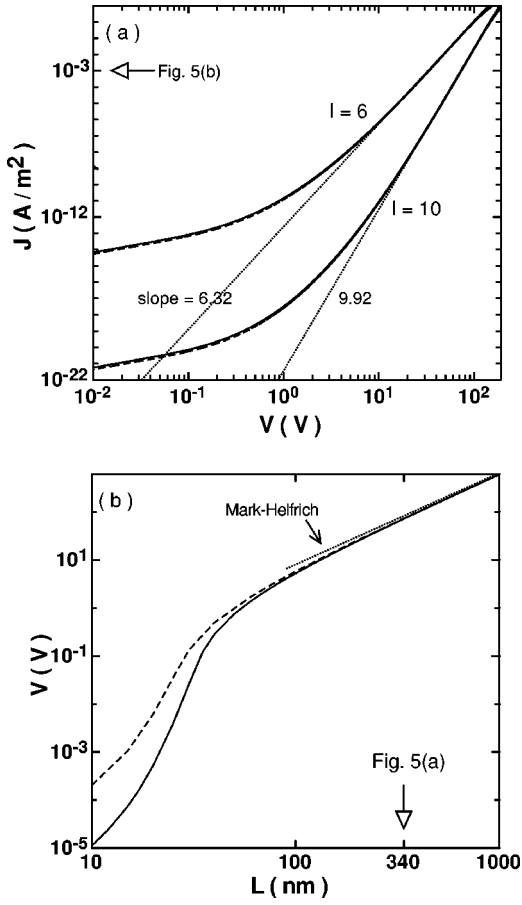


FIG. 5. Electrical properties of a solid with an exponential distribution of traps for a high total trap density  $N_t = 10^{24} \text{ m}^{-3}$ . (a) Current-voltage characteristics. (b) Voltage-thickness characteristics. The definition of dashed and solid curves and all other parameters are the same as in the caption of Fig. 4.

$V$ - $L$  curve follows the same general features of the single trap case. In the high injection regime, however, the region where the voltage increase with the third power of the thickness is less apparent than in Fig. 2(a). This is due to the higher value of  $N_t$  and the lower value of  $n_0$  used to calculate the solid curve in Fig. 4(b), compared to the values used in Fig. 2(a). The interval between  $x_0$  and  $L_{cr}$  is then smaller, and the slope of the solid curve decreases at small thicknesses, where  $L$  approaches  $x_0$  ( $x_0$  is about 1 nm when  $n_0 = 10^{25} \text{ m}^{-3}$  compared to 0.3 nm when  $n_0 = 10^{26} \text{ m}^{-3}$ ).

For thick devices so that  $L \gg x_0$  (dashed curve) or  $L \gg L_{cr}$  (solid curve) the transport properties are dominated by the filling of the traps in the distribution and there is a convergence of the curves calculated assuming different injection regimes. In this limit both curves tend to follow the  $V$ - $L$  dependence predicted by the Mark-Helfrich equation. However, the numerical values of  $V$  are lower than the values obtained by Eq. (8), because the analytical expression was derived assuming that the majority of the injected charge is trapped.

In Fig. 5(a) we repeat the numerical calculations performed in Fig. 4 but assuming a higher density of traps  $N_t = 10^{24} \text{ m}^{-3}$ . The increase of the trap density decreases considerably the magnitude of the current at low applied volt-

ages. Under these circumstances the experimental observation of the diffusion induced Ohms law regime is limited by the resolution of the measurement apparatus. This result can explain why the diffusion-induced regime was observed only in organic devices fabricated and operated under ultrapure UHV conditions,<sup>2</sup> which avoids the formation of injection barriers at the contacts and the presence of a high concentration of impurity-related trap levels in the organic layer. One can also see in Fig. 5(a) that the power-law behavior in the trap-filling region extends over a wider range of values of  $V$  compared to the insulator with low density of traps. The increase in the concentration of the trapping states decreases the fraction of traps filled with carriers injected by diffusion from the contacts. The slopes in Fig. 5(a) approach then the values predicted by Eq. (8), but are still lower than the values determined by this expression. Similar results were obtained from numerical simulations of organic electroluminescent devices with a high concentration of traps and including diffusion.<sup>26</sup> In Ref. 26, however, the lower values of the power factor obtained from the numerical simulation compared to the analytical formula are related to the transport and recombination mechanisms of the double-carrier injection. Here we demonstrate that a similar effect also occurs in a single carrier device.

Figure 5(b) shows the  $V$ - $L$  characteristics for the simulation in Fig. 5(a). The value of  $l$  and the current density level are again the same as for Fig. 3. In this situation  $L_{cr} \approx 10 \text{ nm}$ , and only the detrapping process is visible even in the high injection regime. At thicknesses above 200 nm the trap-limited transport is dominant and both numerical curves in Fig. 4(b) have the same value. They tend to follow a power-law behavior similar to the one determined by Eq. (8), but again with a slightly lower voltage than the value obtained using the analytical theory.

#### IV. CONCLUSIONS

We showed that diffusion effects cannot be neglected in modeling the electrical transport of thin organic solids with trapping centers. Application of the conventional theory of space-charge-limited current to fit experimental data in such systems can lead to incorrect determination of material parameters.

We analyzed several effects that have been ignored in the literature until now.

(1) The space-charge limited current is modified by diffusion when the insulator thickness is below 100 nm.

(2) The density of free charge carriers at the injecting electrodes ( $n_0$ ), compared to the density of traps in the insulator ( $N_t$ ), determines two different regimes of diffusion injection. When  $n_0 \leq N_t$ , low-injection regime, the density of electrons in very thin solids is almost homogeneous and given by  $n_0$ . However, when  $n_0 > N_t$ , a high-injection regime is established. Under this condition there is a range of values of the insulator thickness  $L$  where the density of free electrons in the insulator is independent from  $n_0$ .

(3) A critical thickness can be identified below which diffusion efficiently leads to trap filling, and the solid behaves as a trap-free insulator.

(4) The applied voltage as a function of the thickness of the insulator, plotted over a long range of thicknesses, reveals the presence of a diffusion-induced “detrapping transition” in the bulk of the insulator.

(5) The Mark-Helfrich equation is not valid for thinner insulators with a low concentration of traps because of the filling by diffusion of part of the trapping states in the exponential distribution.

(6) The accumulation of charges near the metal/insulator interface can be a natural consequence of the diffusion from Ohmic contacts and of the limited density of available conducting states in the organic insulator.

These effects are relevant for different aspects of experimental research on insulator-based devices, such as organic light emitting diodes. As an example, it can be noted that a measurement of the “detrapping transition” in the voltage-thickness curve at a constant current, mentioned in point (4), and the consequent determination of the critical length, could be used as a technique to estimate the density of traps in the solid. This technique would be more precise than the deter-

mination of  $N_t$  using the threshold trap-filling voltage in the current-voltage curve.

The last two points are also relevant to current investigations on organic devices. There, the simple theory on space-charge limited current and the Mark-Helfrich equation are widely applied to fit current-voltage characteristics. This can lead to an underestimated density of traps, in the case of one discrete trap level, or a too low characteristic thermal excitation energy of the trap distribution, in the case of an exponential distribution of traps. In addition, charge accumulation has been observed near the interfaces of organic devices but was frequently attributed to the formation of a dipole layer between the organic insulator and the metal electrode. Our work provides an alternative explanation.

#### ACKNOWLEDGMENTS

M.K. would like to thank CNPq and the Nonlinear Optics Laboratory, ETH Zurich, for financial support.

---

\*Present address: Departamento de Engenharia Elétrica, Universidade Federal do Paraná, 81531-9900 Curitiba PR, Brasil.

<sup>1</sup>M. Kiy, P. Losio, I. Biaggio, M. Koehler, A. Trapponier, and P. Günter, *Appl. Phys. Lett.* **80**, 1198 (2002).

<sup>2</sup>M. Kiy, I. Biaggio, M. Koehler, and P. Günter, *Appl. Phys. Lett.* **80**, 4366 (2002).

<sup>3</sup>N. F. Mott and R. W. Gurney, *Electronic Processes in Ionic Crystals* (Oxford, London, 1940).

<sup>4</sup>D. R. Lamb, *Electrical Conduction Mechanisms in Thin Insulating Films* (Methuen, London, 1967).

<sup>5</sup>M. A. Lampert and P. Mark, *Current Injection in Solids* (Academic, New York, 1970).

<sup>6</sup>K. C. Kao and W. Hwang *Electrical Transport in Solids* (Pergamon, Oxford, 1981).

<sup>7</sup>P.E. Burrows, Z. Shen, V. Bulovic, D.M. McCarty, S.R. Forrest, J.A. Cronin, and M.E. Thompson, *J. Appl. Phys.* **79**, 7991 (1996).

<sup>8</sup>M. Stössel, J. Staudigel, F. Steuber, J. Blässing, J. Simmerer, and A. Winnacker, *Appl. Phys. Lett.* **76**, 115 (2000).

<sup>9</sup>M. Stössel, J. Staudigel, F. Steuber, J. Blässing, J. Simmerer, A. Winnacker, H.-H. Johannes, and W. Kowalsky, *Synth. Met.* **111–112**, 19 (2000).

<sup>10</sup>V.I. Arkhipov, P. Heremans, E.V. Emelianova, and G.J. Adriaenssens, *Appl. Phys. Lett.* **79**, 4154 (2001).

<sup>11</sup>T. Mori, S. Miyake, and T. Mizutani, *Jpn. J. Appl. Phys.* **34**, 4120 (1995).

<sup>12</sup>M.W. Klein, D.H. Dunlap, and G.G. Malliaras, *Phys. Rev. B* **64**, 195332 (2001).

<sup>13</sup>J.S. Bonham, *Phys. Status Solidi A* **61**, 1198 (1971).

<sup>14</sup>P. Delannoy, *Eur. J. Appl. Math.* **7**, 13 (1981).

<sup>15</sup>G.G. Roberts and R.H. Tredgold, *J. Phys. Chem. Solids* **25**, 1349 (1964).

<sup>16</sup>M.A. Lampert and F. Edelman, *J. Appl. Phys.* **35**, 2971 (1964).

<sup>17</sup>A. Rosental and A. Sapor, *J. Appl. Phys.* **45**, 2787 (1974).

<sup>18</sup>J. Staudigel, M. Stössel, F. Steuber, and J. Simmerer, *J. Appl. Phys.* **86**, 3895 (1999).

<sup>19</sup>A.B. Walker, A. Kambili, and S.J. Martin, *J. Phys.: Condens. Matter* **14**, 12271 (2002).

<sup>20</sup>M.A. Baldo and S.R. Forrest, *Phys. Rev. B* **64**, 085201 (2001).

<sup>21</sup>H. K. Henisch, *Semiconductor Contacts* (Oxford, London, 1984).

<sup>22</sup>G. Horowitz, D. Fichou, X. Peng, and P. Delannoy, *J. Phys. (France)* **51**, 1489 (1990).

<sup>23</sup>H. Baessler, G. Herrmann, N. Riehl, and G. Vaubel, *J. Phys. Chem. Solids* **30**, 1579 (1969).

<sup>24</sup>H. Scher, M.F. Shlesinger, and J.T. Bendler, *Phys. Today* **44**, 26 (1991).

<sup>25</sup>D.M. Pai and B.E. Springett, *Rev. Mod. Phys.* **65**, 163 (1993).

<sup>26</sup>J. Shen, and J. Yang, *J. Appl. Phys.* **83**, 7706 (1998).